Anisotropic magnetoresistance in a two-dimensional electron system with Rashba and Dresselhaus spin-orbit coupling

C. M. Wang[*]

School of Physics and Electrical Engineering, Anyang Normal University, Anyang 455000, China
(Received 3 June 2010; revised manuscript received 30 September 2010; published 27 October 2010)

We systematically study the anisotropic magnetoresistance (AMR) in a two-dimensional electron system with a combined Rashba and Dresselhaus spin-orbit interaction by exactly solving the kinetic equation. This AMR originates from the combination of spin-orbit coupling and in-plane magnetization, instead of the combined effect of spin-orbit coupling and polarized impurities emphasized in previous theoretical studies. A combined electromagnetic potential is taken into account to investigate the effect of impurity scattering. The electric component of the potential is long ranged, and both the positions and the directions of the magnetic moments of magnetic impurities are random. For long-range electric collision, AMR occurs and AMRs due to remote charged scatterers and background ones are comparable. For pure magnetic scattering, the magnitude of AMR is tiny when the magnetization is smaller than a singular magnetization. However, the anisotropy of spin-spin coupling can enhance the AMR and its magnitude reaches up to nearly 100% when only the majority band is occupied. For the combined electromagnetic potential, the magnitude of AMR is not very large and its sign is always positive when the electric part of scattering is remote. A sudden step of AMR emerges when the value of magnetization is near the Fermi energy, which is due to the uncontinuity of the density of state.

I. INTRODUCTION

The discovery of the anisotropic magnetoresistance (AMR), describing the dependence of electric resistance on the direction of magnetization in magnetic materials, dates back over 150 years.[1] Recently, this phenomenon causes people renewed attention due to the fact that it is related to the spin-orbit coupling (SOC), the key point of the emerging spintronics.[2] In particular, owing to the strong spin-orbit splitting energy and few involved bands,[3] diluted magnetic semiconductor has become one of the favorable systems for AMR investigation.[4–8] In spite of the long history of AMR study, the mechanism of the AMR is still ambiguous. The origin of it is often described vaguely in terms of anisotropic carrier lifetimes. Most of the experimental results are explained based on a phenomenological analysis.[9,10]

Very recently, AMR is investigated in the combined Rashba and Dresselhaus model in the presence of electromagnetic impurity (EMI).[11] It seems that the polarized magnetic impurity is an essential condition for the occurrence of AMR. However, it is found that AMR can also exist in spin-orbit-coupled systems with an in-plane magnetization in the presence of long-range electric collision.[12,13] The combination of SOC and magnetization leads to the anisotropy of group velocity or distribution function, hence, AMR may occur (see the discussion in Sec. II C). Nevertheless, in the presence of short-range spin-independent disorders, the AMR vanishes[14] due to the complete cancellation between the nonvertex and vertex parts of the conductivities when both two spin-orbit coupled bands are occupied.[15] This cancellation is in sharp contrast to the spin-Hall effect, where the cancellation takes place for arbitrary nonmagnetic scattering, but is similar to the anomalous Hall effect[16,17] and the current-induced spin polarization effect[18] in spin-orbit coupled system with an out-of-plane magnetization. It is very interesting that for some transport properties the cancellation

takes place for any nonmagnetic collision while for other properties it is valid only for the short range one in two-dimensional electron gas (2DEG) with SOC.

The *s-d* exchange coupling is the usual form describing the interaction between the magnetic impurity and the carrier in dilute magnetic semiconductor theoretically. The coupling between single impurity and single carrier is given by

$$h_M = J_{ex} s \cdot \widetilde{S}.$$

Here J_{ex} is the exchange strength, s is the carrier's spin, and $\widetilde{S}$ is the spin of the magnetic impurity. In this equation, the spin of carrier is treated as a quantum operator while the impurity's spin is considered to be a classical one. Unfortunately the exchange interaction in dilute magnetic semiconductor is far from being fully understood. The value of coupling strength J_{ex} in dilute magnetic semiconductor is still a subject of debate. The experimental measurement shows that the coupling constant is negative[19] while the first-principles calculation gives a positive value.[20] Furthermore, this exchange model only gives qualitative agreement with the experimental observation.[21] Hence, in this paper we consider one type of anisotropic *s-d* interaction, i.e., the XXZ (or XYZ) interaction, where the in-plane exchange constant is different from the out-of-plane one. Many aspects can induce anisotropic coupling, such as the surface effect, the SOC and the strain, etc. When the magnetic impurity is near the surface of the sample, an anisotropic term with the form $D(\widetilde{S} \cdot \hat{z})^2$ appears.[22] Here D is an anisotropic constant. This anisotropic term is closely related to the XXZ exchange model.[23] The SOC and the strain can induce an effective spin-orbit field. This field causes rotation of the impurity's spin through a angle, leading to the anisotropy of the exchange coupling. For example, if the classical impurity's spin rotate about z axis through a counterclockwise angle γ,

the spin becomes $\widetilde{S}' = (\widetilde{S}_x \cos \gamma - \widetilde{S}_y \sin \gamma, \widetilde{S}_x \sin \gamma + \widetilde{S}_y \cos \gamma, \widetilde{S}_z)$. Therefore, the s-d exchange Hamiltonian becomes the anisotropic one $J_{ex} s \cdot \widetilde{S}' = J_{ex}(\cos \gamma s_x \widetilde{S}_x + \cos \gamma s_y \widetilde{S}_y + s_z \widetilde{S}_z) + \cdots$. In this work we introduce the anisotropy through the phenomenological constants in XXZ (or XYZ) exchange model and do not emphasize a specific microscopic origin of the anisotropy. It is expected to obtain some novel results contrast to the isotropic s-d exchange model and these results could be realized experimentally by tuning the above-mentioned factors. Recently, this XXZ anisotropic exchange model has been used to discuss the spin-Hall effect,[24] anomalous Hall effect,[25] and current-induced spin polarization[26] in magnetic semiconductor, theoretically.

One of the remarkable AMR features in (Ga,Mn)As-diluted magnetic semiconductors is its minus sign of the noncrystalline component,[27,28] i.e., the conductivity parallel to magnetization is larger than perpendicular to magnetization, which is opposite to most metallic ferromagnets. Introducing a "coherent" sum of electric and magnetic scatterings, Rushforth *et al.*[6,29] studied the AMR under the relaxation-time approximation. Both the magnitude and the sign of AMR are found to rely on the relative strength of the nonmagnetic and magnetic contributions of magnetic-ionized Mn acceptors. The destructive interference induced from the combination of electric and magnetic potential when the current is parallel to the magnetization leads to the negative AMR.[30] A maximum AMR magnitude (-200%), originating from vanishing scattering rate, is obtained at certain relative strength of two parts of scattering. In 2DEG with Rashba SOC (Ref. [31]) or combined Rashba and Dresselhaus SOC,[11] exact solution of linear-response Boltzmann equation is obtained to investigate AMR. Similarly, the coherent superposition of electric and magnetic parts, leading to zero scattering probability of one particular state, produces a 200% magnitude AMR when two components have equal strength. One notes that, in the previous theoretical research, the spins of the magnetic impurities are assumed to be fully polarized in the mean-field description, i.e., all the moments of the local magnetic impurities are along a single direction (we refer to it as to the "single-orientation model"). However, in some magnetic materials, where the spins of magnetic impurities are polarized partially, both the positions and the orientations of classical magnetic moments should be randomly distributed. Hence, a complementary study of AMR in this system is highly desirable. It is interesting to see whether the AMR in this partly polarized system could be negative and its magnitude could be large. For this magnetic system, the random magnetic impurities give rise to a finite spontaneous magnetization at the lowest order approximation. This average magnetization acts on the electron spin, leading to an effective Zeeman splitting term in the single-particle Hamiltonian. The remaining effect of magnetic impurities on the collision is modeled by XXZ or XYZ model, describing the interaction between the *effective* impurity spins and the electron spins. This interaction describes the remaining effect of magnetic impurities hence it should be regarded as the effect of effective impurities. The orientations of the *effective* impurity spins are isotropic, hence, in the lowest order, both two models result in zero average exchange fields. These *effective* mag-

netic impurities only have an effect on the relaxation. Therefore, the AMR in this system originates from the combination of SOC and polarized bands. This mechanism is different from the previous studies, where the AMR is due to SOC and polarized impurities.

In this paper, by exactly solving Boltzmann-type kinetic equation, we analyze the AMR of a combined Rashba and Dresselhaus model in the presence of an in-plane spontaneous magnetization and EMI scattering. This model can be applied to discuss the AMR in magnetic material where the magnetic impurities are polarized in part. The AMR of this system has been studied relatively little. Furthermore, the origin of AMR in this paper is significantly different from previous studies. The relatively realistic long-range potential is used to discuss the effect of the electric scattering part. We find that, in such system, the AMR exists even when both bands are occupied and the remote and background impurities have comparable effects on AMR. At the same time, the XXZ model, after taking the average over the directions of local magnetic moments, is applied for the magnetic part of collision. It is found that the AMR is observable only when the magnetization is larger than a singular one. Moreover, it is interesting that the out-of-plane coupling between the electron and impurity spins can enhance the magnitude of AMR drastically. More generally, we also discuss the effect of XYZ model on AMR. Moreover, we numerically investigate the dependence of AMR on the ratio between two scattering contributions of conductivity and find that the magnitude of AMR is not very large for this partly polarized system.

The paper is organized as follows. In Sec. II we derive the kinetic equation for nonequilibrium distribution function in the presence of EMI scattering and discuss the general origin of AMR from the kinetic equation. In Secs. III A–III C, we perform numerical calculations to study AMRs in the presence of pure electric, magnetic, and combined electromagnetic scatterers, respectively. Finally, we conclude our results in Sec. IV.

II. BASIC FORMALISM

A. System and Hamiltonian

We consider a Rashba and Dresselhaus spin-orbit coupled 2DEG in the x-y plane in the presence of an in-plane spontaneous magnetization along x direction $\zeta = (\zeta, 0, 0)$. The single-particle Hamiltonian can be written as

$$\hat{H}_0 = \frac{k^2}{2m} + \alpha(k_y \hat{\sigma}_x - k_x \hat{\sigma}_y) + \beta(k_x \hat{\sigma}_x - k_y \hat{\sigma}_y) - \zeta \hat{\sigma}_x, \quad (1)$$

where α (β) is the Rashba (Dresselhaus) SOC parameter, m is the electron effective mass, $\hat{\boldsymbol{\sigma}} = (\hat{\sigma}_x, \hat{\sigma}_y, \hat{\sigma}_z)$ are the usual Pauli matrices, $\boldsymbol{k} = (k_x, k_y)$ is the two-dimensional electron wave vector. The origin of spontaneous magnetization will be discussed in Sec. II B. By introducing a unitary transformation $U_k = (u_{k1}, u_{k2})$, this Hamiltonian (1) can be diagonalized, $H_0 = U_k^\dagger \hat{H}_0 U_k = \text{diag}(\varepsilon_{k1}, \varepsilon_{k2})$. Here the eigenenergies $\varepsilon_{k\mu}$ and the eigenstates $u_{k\mu}$ of Hamiltonian (1) are given by

$$\varepsilon_{k\mu} = \frac{k^2}{2m} + (-1)^\mu \lambda_k, \quad (2)$$
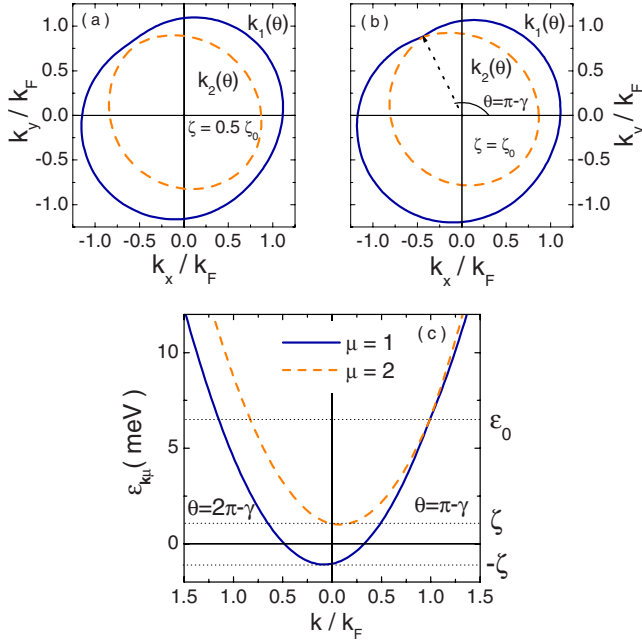
FIG. 1. (Color online) Two Fermi contours $k_\mu(\theta)$ for the magnetizations (a) $\zeta=0.5\zeta_0$ and (b) $\zeta=\zeta_0$. (c) The energy spectra at $\theta=\pi-\gamma$ and $\theta=2\pi-\gamma$ are shown schematically. The relevant material parameters for InAs-based heterojunction are taken as: electron effective mass $m=0.036m_e$ (Ref. 32), the electron density $N=1.0\times10^{11}$ cm^{-2}, and the Rashba and Dresselhaus SOC constants $\alpha=0.2$ eV Å and $\beta=0.1$ eV Å. Here m_e is the free electron mass and $k_F=\sqrt{2\pi N}$ is the Fermi momentum in the absence of SOC and magnetization.

$$u_{k\mu} = \frac{1}{\sqrt{2}}\begin{pmatrix} 1 \\ i(-1)^{\mu+1}e^{i\chi_k} \end{pmatrix}. \quad (3)$$

λ_k is the energy splitting due to the interplay between the SOC and Zeeman term

$$\lambda_k = \sqrt{\eta_\theta^2 k^2 + \zeta^2 - 2\zeta k(\alpha\sin\theta + \beta\cos\theta)},$$

the angle $\chi_k = \tan^{-1}[(\alpha k_y + \beta k_x - \zeta)/(\alpha k_x + \beta k_y)]$, and $\mu=1,2$ with $\eta_\theta^2 = \alpha^2+\beta^2+2\alpha\beta\sin 2\theta$ and θ being the polar angle of momentum k. It should be noted that this unitary transformation changes the system from the spin basis to the helix basis.

It is found that there is a degenerate point at Fermi contours when $\zeta=\zeta_0$ at $\theta=\pi-\gamma$ ($\theta=2\pi-\gamma$) for $\alpha>\beta$ ($\alpha<\beta$) with

$$\zeta_0 = \sqrt{2m\varepsilon_F}\frac{|\alpha^2-\beta^2|}{\sqrt{\alpha^2+\beta^2}}, \quad (4)$$

$$\gamma = \tan^{-1}\frac{\alpha}{\beta}. \quad (5)$$

Here ε_F is the Fermi energy. This feature can be seen clearly in Figs. 1(a) and 1(b), where we show the Fermi contours $k_\mu(\theta)$ for different average magnetizations. For combined Rashba and Dresselhaus model with $\alpha=\beta$, ζ_0 equals zero. In this case, the degeneracy appears at $\theta=3\pi/4$, $7\pi/4$ for zero

magnetization. In Fig. 1(c) the schematic energy spectra at $\theta=\pi-\gamma$ and $\theta=2\pi-\gamma$ are shown, where ε_0 is the energy at the degenerate point. For fixed momentum k, ε_{k2} is always larger than ε_{k1}. It can be seen that for $\varepsilon_F>\zeta$ both the two helix bands are occupied while for $\varepsilon_F<\zeta$ the upper band ($\mu=2$) is depopulated. Analogous to the pure Rashba model,[33] the Fermi energy is nearly a constant, independent of the magnetization, when two helix bands are occupied for this combined Rashba and Dresselhaus model. And the value of it equals the one in the absence of magnetization, ε_F^0, if the electron density is fixed. For high magnetization when only the lower band is occupied, the Fermi energy decreases linearly as $\varepsilon_F\approx 2\varepsilon_F^0-\zeta$. It should be noted that the degenerate magnetization ζ_0 is not proportional to the SOC constant for pure Rashba or Dresselhaus model since the Fermi energy ε_F relies on the SOC strength.

B. Kinetic equation

When the homogenous system is driven by an in-plane dc electric field $E=(E_x,E_y,0)$, the 2×2 matrix Wigner distribution function $\rho(k,T)=-iG^<(k,T,T)$ in the helix basis obeys the following kinetic equation[17]

$$\left(\frac{\partial}{\partial T} - eE\cdot\nabla_k\right)\rho + eE\cdot[\rho, U_k^\dagger\nabla_k U_k] + i[H_0,\rho] = -I_{\rm sc} \quad (6)$$

with the scattering integral in the helix basis

$$I_{\rm sc} = \int_{-\infty}^{T} dt'[\Sigma^r G^< + \Sigma^< G^a - G^r\Sigma^< - G^<\Sigma^a](T,t')(t',T). \quad (7)$$

In this paper, we consider the EMI scattering. The electric scattering originates from the interaction between the electron and the ionized impurity (including the ionized nonmagnetic and magnetic impurities in the quantum well) and a Coulomb interaction is assumed. The magnetic scattering is described by the following XXZ exchange form:

$$\tilde{u}_M(r) = \sum_{\{R_j,\theta_{Mj},\phi_{Mj}\}} J(r-R_j)[s_x\tilde{S}_x(R_j,\theta_{Mj},\phi_{Mj}) + s_y\tilde{S}_y(R_j,\theta_{Mj},\phi_{Mj}) + \Delta s_z\tilde{S}_z(R_j,\theta_{Mj},\phi_{Mj})]. \quad (8)$$

The in-plane coupling between electron spin and impurity spin is assumed to be different from the out-of-plane one. Here $s=\hat{\sigma}/2=(s_x,s_y,s_z)$ is the spin vector of the electron, being treated as a quantum quantity, and $\tilde{S}=(\tilde{S}_x,\tilde{S}_y,\tilde{S}_z)$ is the spin of the classical local magnetic disorder at position R_j. (θ_{Mj},ϕ_{Mj}) denotes the orientation of the magnetic moment. $J(r-R_j)$ is the exchange coupling and Δ is the anisotropic parameter. We assume that the nonzero average spin of magnetic impurity is along the x direction. This average spin results in the above-mentioned spontaneous magnetization and, hence, the magnetic scattering is given by

$$\tilde{u}_{\mathrm{M}}(\boldsymbol{r}) = \sum_{\{\boldsymbol{R}_j, \theta_{\mathrm{M}j}, \phi_{\mathrm{M}j}\}} J(\boldsymbol{r} - \boldsymbol{R}_j)[s_x(\widetilde{S}_x - \langle\widetilde{S}_x\rangle) + s_y\widetilde{S}_y + \Delta s_z\widetilde{S}_z]$$

$$- \hat{\sigma}_x \left[-\frac{1}{2} \sum_{\{\boldsymbol{R}_j, \theta_{\mathrm{M}j}, \phi_{\mathrm{M}j}\}} J(\boldsymbol{r} - \boldsymbol{R}_j)\langle\widetilde{S}_x\rangle \right]$$

$$\equiv u_{\mathrm{M}}(\boldsymbol{r}) - \zeta\hat{\sigma}_x. \tag{9}$$

Here, for shortness, the arguments in impurity's spin $(\boldsymbol{R}_j, \theta_{\mathrm{M}j}, \phi_{\mathrm{M}j})$ are not written out. The *effective* scattering potential $u_{\mathrm{M}}(\boldsymbol{r})$ and the spontaneous magnetization are written as

$$u_{\mathrm{M}}(\boldsymbol{r}) = \sum_{\{\boldsymbol{R}_j, \theta_{\mathrm{M}j}, \phi_{\mathrm{M}j}\}} J(\boldsymbol{r} - \boldsymbol{R}_j)[s_x S_x(\boldsymbol{R}_j, \theta_{\mathrm{M}j}, \phi_{\mathrm{M}j})$$

$$+ s_y S_y(\boldsymbol{R}_j, \theta_{\mathrm{M}j}, \phi_{\mathrm{M}j}) + \Delta s_z S_z(\boldsymbol{R}_j, \theta_{\mathrm{M}j}, \phi_{\mathrm{M}j})], \tag{10}$$

$$\zeta = -\frac{1}{2} \sum_{\{\boldsymbol{R}_j, \theta_{\mathrm{M}j}, \phi_{\mathrm{M}j}\}} J(\boldsymbol{r} - \boldsymbol{R}_j)\langle\widetilde{S}_x\rangle \tag{11}$$

with the spin of the *effective* classical magnetic impurity $\boldsymbol{S}(\boldsymbol{R}_j, \theta_{\mathrm{M}j}, \phi_{\mathrm{M}j}) = (S_x, S_y, S_z) = (\widetilde{S}_x - \langle\widetilde{S}_x\rangle, \widetilde{S}_y, \widetilde{S}_z) = S(\boldsymbol{R}_j)(\sin\theta_{\mathrm{M}j} \cos\phi_{\mathrm{M}j}, \sin\theta_{\mathrm{M}j}\sin\phi_{\mathrm{M}j}, \cos\theta_{\mathrm{M}j})$. The term relating to the spontaneous magnetization is absorbed in the single particle Hamiltonian (1). This magnetic scattering $u_{\mathrm{M}}(\boldsymbol{r})$ describes the remaining contribution of magnetic impurities apart from the contribution to the spontaneous magnetization, hence it should be regarded as the effect of effective impurities and we neglect the word "effective" in the following text. This effective scattering potential is still modeled by the XXZ interaction.[24] Note that this interaction does not break the in-plane symmetry. We also assume that the orientations of these classical magnetic moments are isotropic. Finally, the total EMI scattering potential is given by $u(\boldsymbol{r}) = u_{\mathrm{N}}(\boldsymbol{r}) + u_{\mathrm{M}}(\boldsymbol{r})$ with the electric scattering and magnetic scattering potentials

$$u_{\mathrm{N}}(\boldsymbol{r}) = \sum_{\{\boldsymbol{R}_i\}} v_{\mathrm{N}}(\boldsymbol{r} - \boldsymbol{R}_i), \tag{12}$$

$$u_{\mathrm{M}}(\boldsymbol{r}) = \sum_{\{\boldsymbol{R}_j, \theta_{\mathrm{M}j}, \phi_{\mathrm{M}j}\}} v_{\mathrm{M}}(\boldsymbol{r} - \boldsymbol{R}_j)U_{\mathrm{M}}(\theta_{\mathrm{M}j}, \phi_{\mathrm{M}j}). \tag{13}$$

Here $v_{\mathrm{N}}(\boldsymbol{r} - \boldsymbol{R}_i)$ and $v_{\mathrm{M}}(\boldsymbol{r} - \boldsymbol{R}_j)$ are the electric and magnetic scattering strengths, respectively. $\boldsymbol{R}_i$ is the position of the electric impurity. The 2×2 matrix $U_{\mathrm{M}}(\theta_{\mathrm{M}}, \phi_{\mathrm{M}})$ is written as[24]

$$U_{\mathrm{M}}(\theta_{\mathrm{M}}, \phi_{\mathrm{M}}) = \begin{pmatrix} \Delta\cos\theta_{\mathrm{M}} & \sin\theta_{\mathrm{M}}e^{-i\phi_{\mathrm{M}}} \\ \sin\theta_{\mathrm{M}}e^{i\phi_{\mathrm{M}}} & -\Delta\cos\theta_{\mathrm{M}} \end{pmatrix}. \tag{14}$$

In the presence of partly polarized magnetic disorders, the impurity-averaging technology should include the average over the orientations of the local magnetic moments besides the randomly positions of impurities.[24] Hence, the self-energy in the self-consistent Born approximation in spin basis is described by Fig. 2 with the form

$$\check{\Sigma}(\boldsymbol{k}) = \int \frac{d\Omega_{\mathrm{M}}}{4\pi} \underset{\check{G}(\boldsymbol{q})}{\triangle}$$
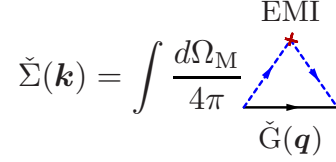
FIG. 2. (Color online) The self-energy in the spin basis in the self-consistent Born approximation for the combined magnetic and electric impurity. The blue dash line denotes the combined scattering potential $v_{\mathrm{T}}(\boldsymbol{k} - \boldsymbol{q}, \theta_{\mathrm{M}}, \phi_{\mathrm{M}})$.

$$\check{\Sigma}^{<,r,a}(\boldsymbol{k}) = \sum_q \int \frac{d\Omega_{\mathrm{M}}}{4\pi} v_{\mathrm{T}}(\boldsymbol{k} - \boldsymbol{q}, \theta_{\mathrm{M}}, \phi_{\mathrm{M}})\check{G}^{<,r,a}(\boldsymbol{q})$$

$$\times v_{\mathrm{T}}(\boldsymbol{k} - \boldsymbol{q}, \theta_{\mathrm{M}}, \phi_{\mathrm{M}}). \tag{15}$$

Here Ω_{M} is the solid angle of the orientation of magnetic moment and the total scattering potential $v_{\mathrm{T}}(\boldsymbol{q}, \theta_{\mathrm{M}}, \phi_{\mathrm{M}})$ is written as

$$v_{\mathrm{T}}(\boldsymbol{q}, \theta_{\mathrm{M}}, \phi_{\mathrm{M}}) = v_{\mathrm{N}}(\boldsymbol{q}) + v_{\mathrm{M}}(\boldsymbol{q})U_{\mathrm{M}}(\theta_{\mathrm{M}}, \phi_{\mathrm{M}}) \tag{16}$$

with $v_{\mathrm{N}}(\boldsymbol{q})$ and $v_{\mathrm{M}}(\boldsymbol{q})$ being the Fourier transforms of $v_{\mathrm{N}}(\boldsymbol{r})$ and $v_{\mathrm{M}}(\boldsymbol{r})$, respectively. In the helix basis, the self-energies $\Sigma^{<,r,a}(\boldsymbol{k}) = U_k^\dagger \check{\Sigma}^{<,r,a}(\boldsymbol{k})U_k$ are given by

$$\Sigma^{<,r,a}(\boldsymbol{k}) = \sum_q \int \frac{d\Omega_{\mathrm{M}}}{4\pi} U_k^\dagger v_{\mathrm{T}}(\boldsymbol{k} - \boldsymbol{q}, \theta_{\mathrm{M}}, \phi_{\mathrm{M}})U_q$$

$$\times G^{<,r,a}(\boldsymbol{q})U_q^\dagger v_{\mathrm{T}}(\boldsymbol{k} - \boldsymbol{q}, \theta_{\mathrm{M}}, \phi_{\mathrm{M}})U_k \tag{17}$$

the expressions of which take complicated forms and are presented in the Appendix A.

To simplify the relaxation term, we use the two-band generalized Kadanoff-Baym ansatz to express the two-time Green's function through the one-time matrix Wigner distribution function.[34] Further, we take the lowest gradient expansion and ignore the collisional broadening. Under the stationary condition, the ρ is independent of the time. To the lowest order of impurity density and electric field, the solution of the kinetic equation can be written as a sum of two terms, $\rho^{\mathrm{I}} + \rho^{\mathrm{II}}$. The first term, ρ^{I}, is collision unrelated and off-diagonal with the elements

$$\rho_{12}^{\mathrm{I}}(\boldsymbol{k}) = \rho_{21}^{\mathrm{I}}(\boldsymbol{k}) = \frac{e\boldsymbol{E}\cdot\nabla_k\chi_k}{4\lambda_k}[n_{\mathrm{F}}(\varepsilon_{k1}) - n_{\mathrm{F}}(\varepsilon_{k2})]. \tag{18}$$

Here $n_{\mathrm{F}}(x)$ is the Fermi-Dirac distribution function. This distribution, relating to the interband transition between two unperturbed helix bands, makes no contribution to charge transport for this system.[12] The collision-related distribution function ρ^{II} is determined by the coupled equations

$$e\boldsymbol{E}\cdot\nabla_k n_{\mathrm{F}}(\varepsilon_{k\mu}) = \pi\sum_{q\mu'}\Lambda_{\mu\mu'}(\boldsymbol{k}, \boldsymbol{q})[\rho_{\mu\mu}^{\mathrm{II}}(\boldsymbol{k}) - \rho_{\mu'\mu'}^{\mathrm{II}}(\boldsymbol{q})]$$

$$\times \delta(\varepsilon_{k\mu} - \varepsilon_{q\mu'}), \tag{19}$$

$$4\lambda_k \operatorname{Re} \rho_{12}^{\mathrm{II}}(\boldsymbol{k}) = \pi \sum_{q\mu\mu'} \bar{\Lambda}_{\mu\mu'}(\boldsymbol{k},\boldsymbol{q})[\rho_{\mu\mu}^{\mathrm{II}}(\boldsymbol{k}) - \rho_{\mu'\mu'}^{\mathrm{II}}(\boldsymbol{q})]$$
$$\times \delta(\varepsilon_{k\mu} - \varepsilon_{q\mu'}). \quad (20)$$

The scattering-related quantities $\Lambda_{\mu\mu'}$ and $\bar{\Lambda}_{\mu\mu'}$ are expressed as

$$\Lambda_{\mu\mu'}(\boldsymbol{k},\boldsymbol{q}) = v_{\mathrm{N}}^2(\boldsymbol{k}-\boldsymbol{q})[1 + (-1)^{\mu+\mu'} \cos(\chi_k - \chi_q)]$$
$$+ \frac{1}{3}v_{\mathrm{M}}^2(\boldsymbol{k}-\boldsymbol{q})[2 + \Delta^2 - (-1)^{\mu+\mu'}\Delta^2$$
$$\times \cos(\chi_k - \chi_q)], \quad (21)$$

$$\bar{\Lambda}_{\mu\mu'}(\boldsymbol{k},\boldsymbol{q}) = (-1)^{\mu'}\frac{1}{3}[3v_{\mathrm{N}}^2(\boldsymbol{k}-\boldsymbol{q}) - \Delta^2 v_{\mathrm{M}}^2(\boldsymbol{k}-\boldsymbol{q})]$$
$$\times \sin(\chi_k - \chi_q). \quad (22)$$

It is obvious that the above coupled Eqs. (19) and (20) agree with the previous study in the absence of magnetic impurities.[12] It is important to note that, for this system in the presence of partly polarized magnetic impurities, the solid angle integral makes the cross terms of v_{N} and v_{M} vanishing in the $\Lambda_{\mu\mu'}$ and $\bar{\Lambda}_{\mu\mu'}$. Hence, the coherent scattering feature does not occur for this XXZ model. In fact, if the XXZ model is replaced by a general XYZ model for the magnetic scattering, the coherent scattering also does not take place after the average over orientations, which can be seen in Appendix B. Accordingly, the coherent sum of scattering operators may be a specialty for single-orientation model.

C. AMR

In the clean limit approximation, the off-diagonal elements of distribution $\rho^{\mathrm{II}}(\boldsymbol{k})$ make no contribution to the drift velocity for this in-plane configuration considered here.[12] At the same time, the off-diagonal elements of the velocity operator play no role in the charge transport, in contrast to the out-of-plane configuration.[17] Therefore, the drift velocity $\boldsymbol{v}_d$ reads

$$\boldsymbol{v}_d = \frac{1}{N}\sum_{k,\mu} \boldsymbol{v}_{k\mu}\rho_{\mu\mu}^{\mathrm{II}}(\boldsymbol{k}) \quad (23)$$

with the group velocity $\boldsymbol{v}_{k\mu} = \nabla_k \varepsilon_{k\mu}$.

Further, we can divide the distribution $\rho_{\mu\mu}^{\mathrm{II}}$ into two parts, $\rho_{\mu\mu}^{\mathrm{II}} = \rho_{\mu\mu}^x E_x + \rho_{\mu\mu}^y E_y$, with $\rho_{\mu\mu}^i (i=x,y)$ independent of the electric field. Substituting $\rho_{\mu\mu}^{\mathrm{II}}$ into the equation of diagonal distributions Eq. (19), we arrive at

$$e\frac{\partial n_{\mathrm{F}}(\varepsilon_{k\mu})}{\partial k_i} = \pi\sum_{q\mu'} \Lambda_{\mu\mu'}(\boldsymbol{k},\boldsymbol{q})[\rho_{\mu\mu}^i(\boldsymbol{k}) - \rho_{\mu'\mu'}^i(\boldsymbol{q})]$$
$$\times \delta[\varepsilon_{k\mu} - \varepsilon_{q\mu'}]. \quad (24)$$

Accordingly, the conductivity tensor

$$\sigma_{ij} = -e\sum_{k,\mu} v_{k\mu}^i \rho_{\mu\mu}^j(\boldsymbol{k}) \quad (25)$$

with the index $j=x,y$, and $v_{k\mu}^i$ as the ith component of group velocity $\boldsymbol{v}_{k\mu}$.

The AMR is defined as

$$\mathrm{AMR} = 2\frac{\rho_{\parallel} - \rho_{\perp}}{\rho_{\parallel} + \rho_{\perp}}, \quad (26)$$

where $\rho_{\parallel}$ and $\rho_{\perp}$ are the longitudinal resistivities for current parallel and perpendicular to the magnetization, respectively. In this paper, we fix the direction of the magnetization (along x axis). In order to obtain the current parallel to the magnetization, one should adjust the electric field so that $J_x = \sigma_{xx}E_x^{\parallel} + \sigma_{xy}E_y^{\parallel} \neq 0$ and $J_y = \sigma_{yx}E_x^{\parallel} + \sigma_{yy}E_y^{\parallel} = 0$ with J_i as the ith component of current and $\boldsymbol{E}^{\parallel} = (E_x^{\parallel}, E_y^{\parallel}, 0)$ denoting the corresponding electric field. Therefore, the J_x is written as

$$J_x = (\sigma_{xx}\sigma_{yy} - \sigma_{xy}\sigma_{yx})E_x^{\parallel}/\sigma_{yy}. \quad (27)$$

At the same time, the longitudinal resistivity for current parallel to the magnetization is expressed as

$$\rho_{\parallel} = \frac{E_x^{\parallel}}{J_x} = \frac{\sigma_{yy}}{\sigma_{xx}\sigma_{yy} - \sigma_{xy}\sigma_{yx}}. \quad (28)$$

On the other hand, the longitudinal resistivity for current perpendicular to the magnetization is given by

$$\rho_{\perp} = \frac{\sigma_{xx}}{\sigma_{xx}\sigma_{yy} - \sigma_{xy}\sigma_{yx}}. \quad (29)$$

Hence, AMR is written as

$$\mathrm{AMR} = -2\frac{\sigma_{xx} - \sigma_{yy}}{\sigma_{xx} + \sigma_{yy}}. \quad (30)$$

In the absence of magnetization, it is found that the x component of the velocity $v_\mu^x(k_x, k_y)$ becomes the y component $v_\mu^y(k_y, k_x)$ when we make the transformation $k_x \leftrightarrow k_y$. Note that, for the sake of convenience, $v_{k\mu}^i$ have been rewritten as $v_\mu^i(k_x, k_y)$, so also do other quantities in the following paragraphs. At the same time, $\cos\chi_k$ exchanges with $\sin\chi_k$ under this transformation. From the fact that $\Lambda_{\mu\mu'}(\boldsymbol{k},\boldsymbol{q})$ depends on $\chi_k - \chi_q$ through the cosine function, $\rho_{\mu\mu}^x(k_x, k_y)$ becomes $\rho_{\mu\mu}^y(k_y, k_x)$ under the transformation $k_x \leftrightarrow k_y$ and $q_x \leftrightarrow q_y$ in Eq. (24). Here we have assumed that the scattering potentials v_{N} and v_{M} only rely on the magnitude of the momentum $\boldsymbol{k}-\boldsymbol{q}$. On the other hand, the exchange of the components of momentum $\boldsymbol{k}$ does not change the integral, Eq. (25). As a result, $\sigma_{xx} = \sigma_{yy}$ and AMR vanishes even in the presence of magnetic disorders, which is modeled by XXZ model. This result is different from the case when the magnetic impurities are fully polarized,[11] where the polarized impurities break the in-plane symmetry and the scattering probability function may depend on $\chi_k + \chi_q$ through a cosine or sine function. Hence $\rho_{\mu\mu}^x(k_x, k_y) \neq \rho_{\mu\mu}^y(k_y, k_x)$, resulting in nonvanishing AMR in the absence of magnetization. For XYZ model in the absence of magnetization, the AMR exists due to the similar reason, which is presented in Appendix B. In this case, though the relation $v_\mu^x(k_x, k_y) = v_\mu^y(k_y, k_x)$ is still satisfied, the symmetrical relation $\rho_{\mu\mu}^x(k_x, k_y) = \rho_{\mu\mu}^y(k_y, k_x)$ is broken.

For another situation when the 2DEG is in the absence of spin-orbit interaction ($\alpha = \beta = 0$), thus $\lambda_k = \zeta$ and $\chi_k = -\pi/2$. It is obvious that $v_\mu^x(k_x, k_y) = v_\mu^y(k_y, k_x)$ and $\rho_{\mu\mu}^x(k_x, k_y)$

$=\rho_{\mu\mu}^{y}(k_y,k_x)$. Hence, AMR also vanishes for the system in the absence of SOC. Note that this argument is valid even when the magnetization is so large that only the lower band is occupied and for the situation in the presence of magnetic disorders.

Therefore, AMR is an effect which can also be induced by the combination of the SOC and magnetization in addition to the combination of SOC and polarized impurity. The combined effect breaks the symmetrical relation $v_{\mu}^{x}(k_x,k_y)$ $=v_{\mu}^{y}(k_y,k_x)$ or the other relation $\rho_{\mu\mu}^{x}(k_x,k_y)=\rho_{\mu\mu}^{y}(k_y,k_x)$. For the present work in the presence of both SOC and magnetization, $\varepsilon_{\mu}(k_x,k_y) \neq \varepsilon_{\mu}(k_y,k_x)$ and $v_{\mu}^{x}(k_x,k_y) \neq v_{\mu}^{y}(k_y,k_x)$. Further, $\Lambda_{\mu\mu'}(k_x,k_y;q_x,q_y) \neq \Lambda_{\mu\mu'}(k_y,k_x;q_y,q_x)$, leading to $\rho_{\mu\mu}^{x}(k_x,k_y) \neq \rho_{\mu\mu}^{y}(k_y,k_x)$. Therefore, AMR may exist even for the nonmagnetic disorders.[12,13] Nevertheless, for short-range nonmagnetic disorders, the vertex part of the conductivity cancels the nonvertex part completely, leading to vanishing AMR, when both two bands are occupied.[15] Note that this cancellation is not valid when the Fermi energy only crosses the lower helix band and AMR appears even for this momentum-independent nonmagnetic scattering.[15,33]

III. NUMERICAL RESULTS

A. Pure electric impurities

To investigate the effect of electric disorders on the AMR, we perform a numerical evaluation in the InAs-based quantum well. We consider contribution from a mixture of the remote and background impurities. The remote scattering is due to ionized remote impurities distributing within a narrow space charge layer with a concentration N_I at a distance s from the interface while the background charged disorders distribute uniformly throughout InAs region with a volume density n_I. The scattering potential can be found in Ref. 35. The material parameters used in this calculation are:[36] the low-frequency dielectric constant $\kappa = 15.54$, the depletion layer charge number density $N_{dep} = 2 \times 10^{10}$ cm^{-2}. The electron effective mass at the band bottom and electron density are the same as those in Fig. 1.

In Fig. 3, we plot the AMRs due to electric remote disorders, background charged impurities, and the mixture of these two types of impurities as functions of magnetization for pure Rashba model. It is evident that for this momentum-dependent electric scattering, all of the AMRs are nonvanishing and these values are comparable. Notice that the calculated AMR either due to remote collision or due to background one is independent of the impurity density. The total AMR is obtained by assuming equal conductivity contributions from two nonmagnetic scattering mechanisms at zero magnetization. Let $n_I = cN_I \times 10^8$ m^{-1} with c as a dimensionless constant. We numerically determine the constant so that the conductivity contributions equal each other. Hence the obtained total AMR is also irrelevant to the remote disorder density N_I. For comparison, we also compute the AMR for δ shape short-range collision by replacing the potential $v_N(\boldsymbol{k}-\boldsymbol{q})$ by the momentum-independent one v_0, which has been shown in the form of thin wine solid line. For these four Rashba SOC constants $\alpha = 0.1, 0.2, 0.3, 0.4$ eV Å, it is found that Fermi energy, ε_F
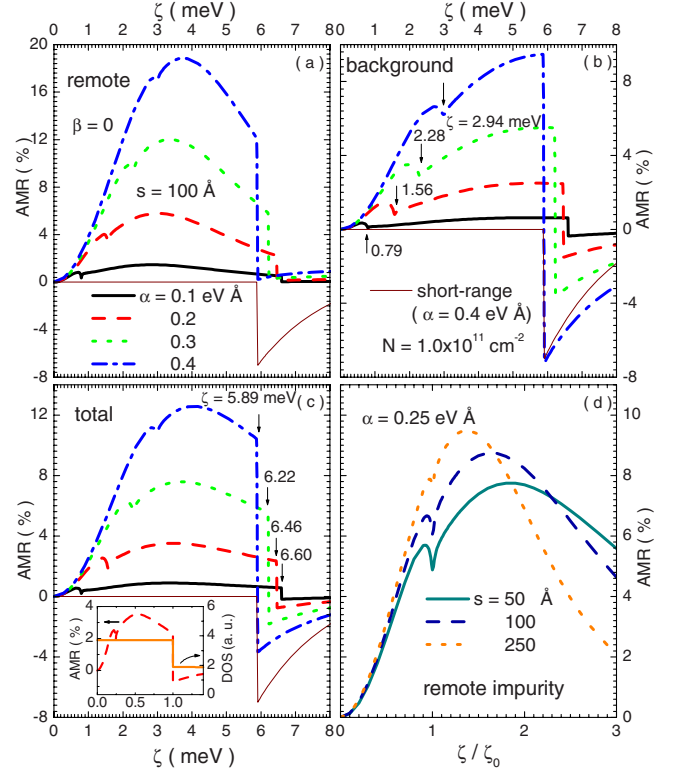
FIG. 3. (Color online) Calculated magnetization dependencies of AMRs in an InAs-based quantum well due to (a) electric remote ionized dopants, (b) background charged impurities, and (c) the mixture of these two types for different Rashba constants. The total AMR due to the mixture is obtained by assuming equal conductivity contributions from both scattering mechanisms at zero magnetization. The thin wine line is calculated for the short-range case with $\alpha = 0.4$ eV Å. Inset of (c) shows the total AMR (red dash line) and corresponding density of state at Fermi energy (orange solid line) when the Rashba constant $\alpha = 0.2$ eV Å, where the horizontal coordinate is ζ/ε_F. (d) AMR induced by remote impurity scattering versus the normalized magnetization for different impurity distances when the Rashba parameter $\alpha = 0.25$ eV Å. Here the electron density $N = 1.0 \times 10^{11}$ cm^{-2}.

$=6.60, 6.46, 6.22, 5.89$ meV, and the singular magnetization, $\zeta_0 = 0.79, 1.56, 2.28, 2.94$ meV, respectively.

It is seen that there is a sudden step in the AMR around $\zeta \approx \varepsilon_F$ both for short-range and long-range electric scattering. AMR vanishes completely for this short-range electric scattering when the Fermi energy crosses both two bands in contrast to the long-range case. The step is due to the van-Hove singularity in the density of state (DOS). The DOS for this two bands model is defined as

$$D(E) = \sum_{\boldsymbol{k}\mu} \delta(E - \varepsilon_{\boldsymbol{k}\mu}). \qquad (31)$$

In the inset of Fig. 3(c), we show the magnetization dependencies of total AMR and DOS at Fermi energy $D(\varepsilon_F)$. The position of the sudden step in AMR is in complete accord with the one of DOS. At the band edge of the $\mu = 2$ band, $\partial\varepsilon_{\boldsymbol{k}\mu}/\partial k \approx 0$, leading to this remarkable structure, which can be confirmed from the schematic energy spectra Fig. 1(c).

Due to the fact that when both bands are occupied, the Fermi energy is almost independent of the magnetization, the DOS at Fermi energy is nearly a constant at $\zeta < \varepsilon_F$. The DOS at $\zeta > \varepsilon_F$ actually depends on the magnetization but the variation is so small that it is almost invisible. The AMR due to the remote disorders is always positive even at $\zeta > \varepsilon_F$, in vivid contrast against with the case of background disorders. For background scattering, the AMR becomes negative at $\zeta > \varepsilon_F$, and the AMRs at $\zeta > \varepsilon_F$ and $\zeta < \varepsilon_F$ are of the same order of magnitude, leading to negative total AMR at $\zeta > \varepsilon_F$.

When both two bands are occupied ($\zeta < \varepsilon_F$), except for the small magnetization-dependent behavior near the regime $\zeta = \zeta_0$, AMR first increases, and then decreases with the increment of the magnetization for remote collision, while the AMR always increases for background electron-impurity scattering. The magnitudes of all these AMRs enhance with increasing the Rashba SOC strength. The value of the AMR induced by remote collision is larger than the one of the background scattering for $\zeta < \varepsilon_F$. The background collision suppresses the magnitude of the total AMR but the behavior of the total one is similar to the AMR due to remote collision. The small magnetization-dependent behavior near ζ_0 arises from the degeneracy of Fermi contours when $\zeta = \zeta_0$ and $\theta = \pi - \gamma$ or $2\pi - \gamma$. Hence, strong interband transition occurs at this point. One notes that the existence of the degenerate point also leads to novel properties of current-induced spin polarization.[37] Near the degenerate point, all of the AMRs first decreases slightly and then increases with the magnetization.

Further, to demonstrate the impurity-distance-related feature of AMR for remote collision at $\zeta < \varepsilon_F$, we plot AMRs as functions of normalized magnetization ζ / ζ_0 for various impurity distances in Fig. 3(d). It is seen obviously that the distance of the remote dopants affects the magnitude of AMR, strongly. With increasing the degree of smoothness of potential, the maximum of AMR increases and a redshift of the AMR peak occurs. At the same time, one also finds that the increasing distance suppresses the small magnetization-dependent behavior near the degenerate point. This is the reason why we did not observe this small feature in our previous study,[12] where we chose a relative large impurity distance.

We now explore the effect of Dresselhaus SOC on AMR in the presence of electric collision. In Fig. 4, we plot the AMRs due to remote collision and the singular magnetization ζ_0 as functions of Rashba SOC strength for fixed Dresselhaus SOC constant $\beta = 0.2$ eV Å when the Fermi energy crosses two bands. In the presence of short-range electric scattering, AMR still vanishes completely for this combined Rashba-Dresselhaus model. Nevertheless, AMR exists, and significantly relies on the SOC parameters for momentum-dependent remote collision. The sign of AMR depends on the ratio α / β and AMR completely vanishes for $\alpha = \beta$ even in the presence of long-range scattering. This is similar to the single-orientation model,[11] though here the scattering is totally electric. For the situation ($\alpha = \beta$), $\varepsilon_\mu(k_x, k_y) = \varepsilon_\mu(k_y, k_x)$, $v_\mu^x(k_x, k_y) = v_\mu^y(k_y, k_x)$, and $\chi(k_x, k_y) = \chi(k_y, k_x)$. At the same time $\rho_{\mu\mu}^x(k_x, k_y)$ becomes $\rho_{\mu\mu}^y(k_y, k_x)$ when we make the transformation $k_x \leftrightarrow k_y$. Hence, $\sigma_{xx} = \sigma_{yy}$.
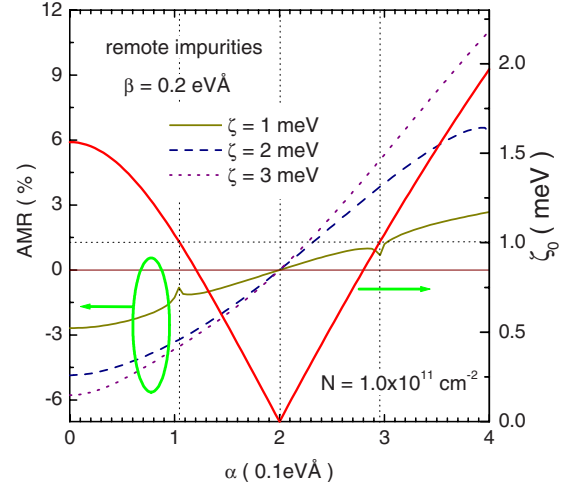
FIG. 4. (Color online) Calculated AMRs due to remote impurities for different magnetizations and the singular magnetization ζ_0 are shown as functions of Rashba SOC strength when $\zeta < \varepsilon_F$. The thin wine lines are obtained for δ-form short-range nonmagnetic collision when the magnetization $\zeta = 3$ meV. Here the Dresselhaus SOC constant $\beta = 0.2$ eV Å. The other parameters are the same as in Fig. 3.

It should be noted that this argument is also valid in the regime when only one band is occupied and for magnetic scattering. Therefore, AMR vanishes for $\alpha = \beta$ even when the magnetization is very large. We mention again that for the situation when both helix bands are occupied, the Fermi energy is nearly independent of the magnetizations.[33] Hence, the singular magnetization is irrelevant to the magnetization. In the parameter regime, $\alpha < 0.4$ eV Å, it is found that the singular magnetization $\zeta_0 < 2$ meV. Hence, near the regime $\zeta_0 = 1$ meV, there exist small variations for AMR when the magnetization $\zeta = 1$ meV. When $\alpha = 0.4$ eV Å, ζ_0 is very close to 2 meV. Therefore, AMR begins to decrease for $\alpha \approx 0.4$ eV Å when the spontaneous magnetization $\zeta = 2$ meV. Note that here the plotted AMR is in the regime $\zeta < \varepsilon_F$. We also calculate the AMR when only majority band is occupied. It is found that, for fixed Dresselhaus SOC parameter, AMR increases monotonously with the Rashba constant from negative to positive for remote scattering.

B. Pure magnetic impurities

Now we concentrate on the AMR due to pure magnetic impurities by assuming momentum-independent scattering strength, i.e., $v_M = v_0$. The calculated AMRs for pure Rashba model, which is irrelevant to the scattering strength, are plotted in Figs. 5 and 6.

It should be noted that the XXZ model does not break the in-plane symmetry for the system in the absence of magnetization. Hence, the anisotropy in conductivity vanishes completely for vanishing magnetization. Actually, the distribution $\rho_{\mu\mu}^i(\boldsymbol{k})$ for this pure Rashba model in the absence of magnetization can be obtained analytically from Eq. (24)
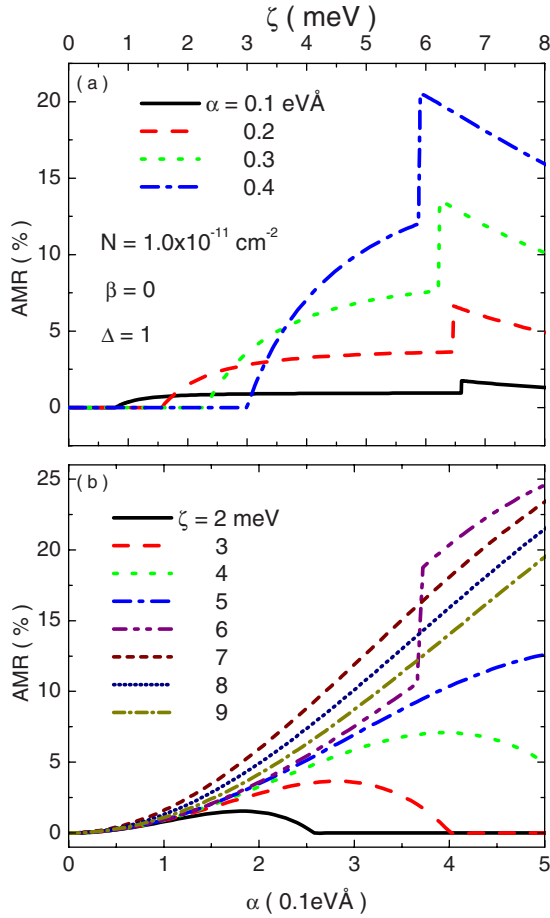
FIG. 5. (Color online) Anisotropy in the conductivity due to pure magnetic disorders described by the anisotropic XXZ interaction are shown as functions of (a) magnetization and (b) Rashba SOC strength, when $\Delta = 1$. Here the Dresselhaus SOC constant $\beta = 0$ and the electron density $N = 1.0 \times 10^{-11}$ cm^{-2}.

$$\begin{bmatrix} \rho_{\mu\mu}^x(\boldsymbol{k}) \\ \rho_{\mu\mu}^y(\boldsymbol{k}) \end{bmatrix} = \frac{e}{v_0^2} \frac{3}{3\Delta^4 + 10\Delta^2 + 8}$$

$$\times \left[\frac{\Delta^2}{m^2} k - \frac{4(1+\Delta^2)}{m} \sqrt{\alpha^2 + \frac{2\varepsilon_F}{m}} \right]$$

$$\times \begin{bmatrix} \cos\theta \\ \sin\theta \end{bmatrix} \delta(\varepsilon_{k\mu} - \varepsilon_F). \qquad (32)$$

Based on the fact that $v_{k\mu}^x \propto \cos\theta$ and $v_{k\mu}^y \propto \sin\theta$, it is found that $\sigma_{xx} = \sigma_{yy}$ and AMR equals zero completely. Note that this is invalid for a general XYZ model, which could be seen in Appendix B. For XXZ model, in the presence of small magnetization $\zeta < \zeta_0$, AMR is so small that it is almost invisible, the variation in which near the regime $\zeta \approx \zeta_0$ is given in the inset of Fig. 6(a). Similarly, the current-induced spin polarization is also tiny when the spontaneous magnetization is smaller than a singular magnetization.[37] We should note that though we discuss the pure Rashba model, AMR also equals zero in the absence of magnetization for the combined Rashba and Dresselhaus model meanwhile it is tiny when $\zeta < \zeta_0$. For the magnetization $\zeta_0 < \zeta < \varepsilon_F$, AMR increases mo-
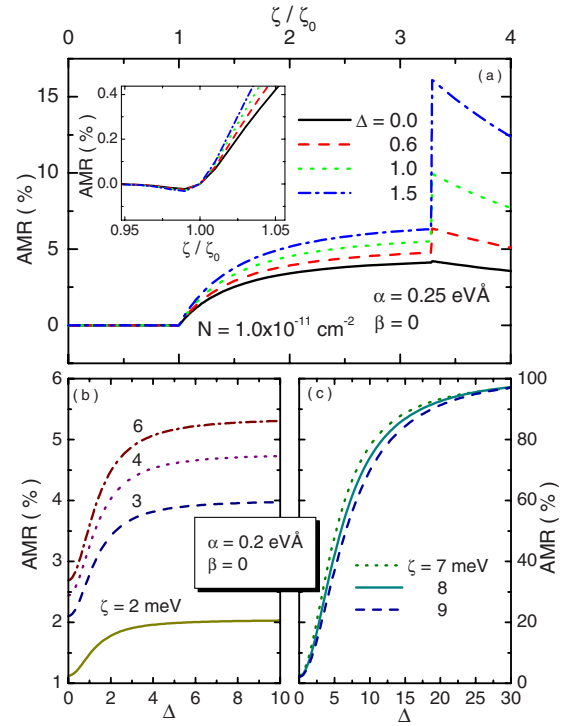
FIG. 6. (Color online) (a) AMRs with the changes of the magnetization for different anisotropic coefficients Δ when the Rashba SOC constant $\alpha = 0.25$ eV Å. The inset shows AMRs for different Δ near the regime $\zeta \approx \zeta_0$. Calculated AMRs as functions of anisotropic parameter Δ when the Fermi energy crosses (a) two bands and (c) one band for the SOC constants $\alpha = 0.2$ eV Å and $\beta = 0$. The other parameters are the same as those in Fig. 5.

notonously, which could be seen in Fig. 5(a). Near the regime $\zeta \approx \varepsilon_F$, the pronounced step structure is also observed for magnetic disorders such as the electric ones. Then AMR decreases gradually and becomes stable for large magnetization when only the majority band is occupied. In Fig. 5(b), the AMRs of the pure Rashba model are shown as functions of Rashba strength for variant magnetizations. Note that for weak magnetization $\zeta < \varepsilon_F$, though the Fermi energy decreases with the SOC, the singular magnetization ζ_0 still increases with the increment of Rashba coupling. As a result, AMR may increase first, then decrease, and even nearly vanish when $\zeta < \zeta_0$, such as $\zeta = 2, 3$ meV. At the same time, in Fig. 5(b) an abrupt increase in AMR with increasing the coupling α for $\zeta = 6$ meV is seen. This feature can be understood due to the fact that with increasing the α, the Fermi energy descends, and when it equals the magnetization, the sudden increase occurs. For large magnetization ($\zeta > \varepsilon_F$), such as $\zeta = 7, 8, 9$ meV, AMR always enhances with ascending the α. For low spin-orbit splitting $m\alpha^2/\zeta \ll 1$ and not very large anisotropic constant $\Delta^2 m\alpha^2/\zeta \ll 1$, the AMR of this single band case is obtained as

$$\text{AMR} = \left(1 + \frac{3}{4}\Delta^2 \frac{\varepsilon_F + \zeta}{\zeta}\right) \frac{m\alpha^2}{\zeta}. \qquad (33)$$

The derivation is very cumbersome and we give it in the Appendix C. The above result shows that AMR decreases
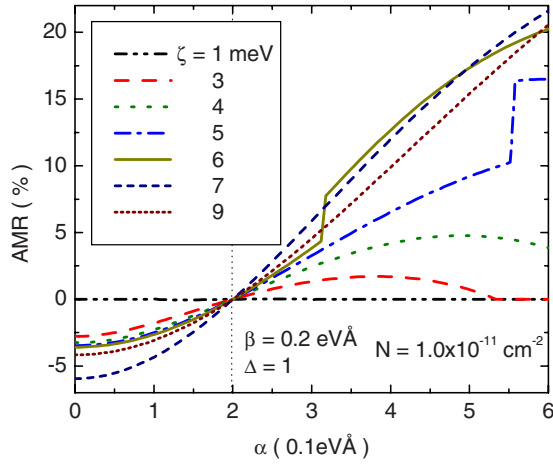
FIG. 7. (Color online) AMR due to isotropic magnetic impurities ($\Delta=1$) for different magnetizations is plotted as a function of Rashba SOC strength when $\beta=0.2$ eV Å.

with the magnetization and increases with anisotropic coupling, which agrees with our numerical results completely.

Further, to demonstrate the effect of anisotropic parameter Δ on the AMR, AMRs for various Δ are plotted in Fig. 6(a). It is seen that the step near $\zeta \approx \epsilon_F$ becomes remarkable with enhancing the anisotropy Δ. For vanishing anisotropy, the sudden increase of AMR almost cannot be observed. In Figs. 6(b) and 6(c), the AMRs are plotted as functions of the anisotropic parameter for $\zeta < \varepsilon_F$ and $\zeta > \varepsilon_F$, respectively. For both two situations, the AMR increases with enhancing the anisotropy, and finally saturates. However, the saturation value and the corresponding anisotropy when AMR begin to saturate are evidently different. Especially, when only one band is occupied, the saturation value of AMR is nearly 100%.

For the combined Rashba and Dresselhaus model, the sign of AMR also relies on the ratio α/β for the magnetic disorders and vanishes when $\alpha=\beta$, which can be seen in Fig. 7. For low magnetization ($\zeta=1$ meV), the AMR is very small and almost invisible. Note that this value is smaller than the one for electric long-range scattering. Hence, in order to obtain observable AMR, one has to apply relative large magnetization. Also an abrupt increase of AMR near the regime $\zeta \approx \varepsilon_F$ is observed for $\zeta=5,6$ meV. When $\zeta > \varepsilon_F$, the AMR ascends with SOC and descends with magnetization, monotonously.

C. Combined electric and magnetic impurities

We now investigate the AMR when the electrons are scattered by the EMIs. The calculated results are summarized in Figs. 8–10. In Fig. 8 we plotted the AMR induced by the combined electric and magnetic disorders as functions of magnetizations. Here the magnetic scattering is taken to be isotropic, i.e., $\Delta=1$. The considered electric scattering is due to (a) remote disorders and (b) momentum-independent short-range one. In the calculation, we have assumed the equal contributions of longitudinal conductivity in the absence of magnetization due to electric or magnetic scattering,
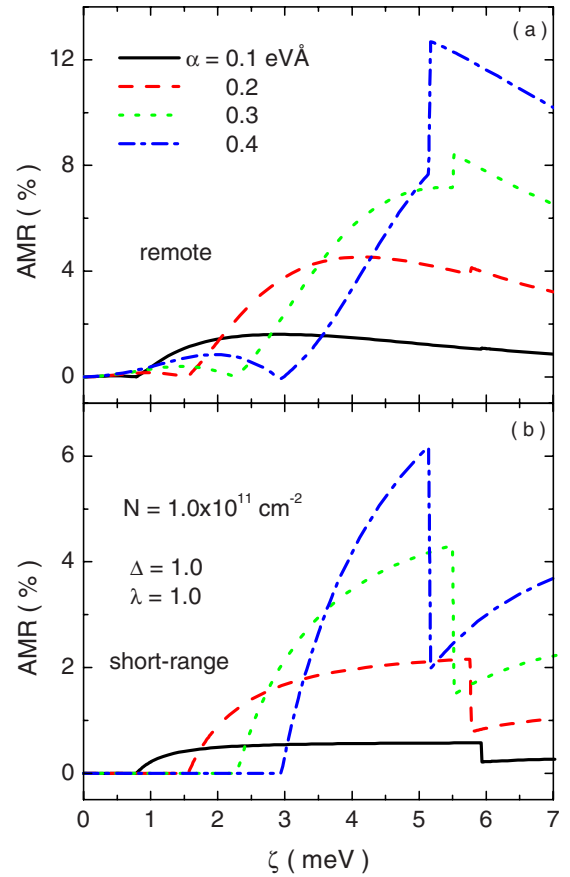
FIG. 8. (Color online) AMR due to EMIs is shown as a function of magnetization for different Rashba SOCs when $\Delta=1$ and $\lambda=1$. Here the considered electric scattering is due to (a) remote disorders or (b) momentum-independent short-range disorders.

i.e., $\lambda=\sigma_N/\sigma_M=1$. Here σ_N and σ_M are the longitudinal conductivities induced by the pure electric and magnetic disorders for vanishing magnetization. It is seen evidently that the AMR is always positive even in the presence of this combined disorders and its magnitude is not very large. For $\zeta < \zeta_0$, the long-ranged electric part of the scattering potential, unlike the short-range one, plays a significant role on the AMR, bringing about the nonzero AMR. Near the regime $\zeta \approx \varepsilon_F$, a sudden increase occurs in the presence of remote electric scattering part, while a sudden decrease emerges for short-range one. This can be understood from the fact that when $\zeta > \epsilon_F$ the magnetic scattering dominates in the AMR induced by combined remote electric and magnetic impurities. However, AMRs due to short-range pure electric and magnetic disorders are of the same order of magnitude. Hence, a competition occurs, leading to different behavior. For $\zeta > \epsilon_F$, it is seen that the total AMR descends with magnetization when the electric part of scattering is remote, unlike the short-ranged one. Note that the step near $\zeta \approx \varepsilon_F$ is very small for the weak SOC case when the electric part of scattering is remote.

It is noted that, for single-orientation model, the AMR may becomes 200% when the ratio between the electric and magnetic parts of the potential equals one.[11] To investigate this ratio-dependent feature for our case, we plot the AMRs
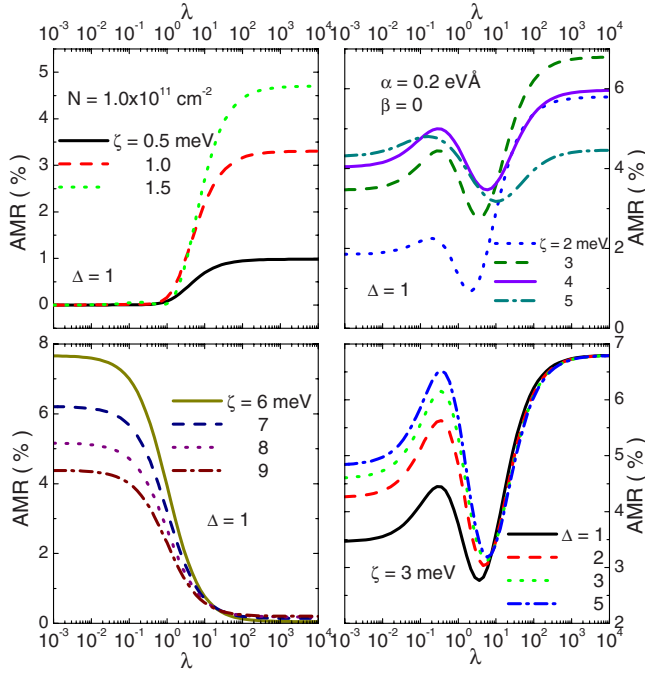
FIG. 9. (Color online) AMR is plotted as a function of the ratio of the longitudinal conductivity σ_N due to remote electric disorders to the conductivity σ_M due to magnetic impurities for the magnetizations (a) $\zeta < \zeta_0$, (b) $\zeta_0 < \zeta < \varepsilon_F$, and (c) $\zeta > \varepsilon_F$. Here the distance of the remote disorders $s = 100$ Å and the anisotropic coupling constant $\Delta = 1$. (d) AMR is shown as a function of the ratio λ for different anisotropic parameters at fixed magnetization.

as functions of ratio λ in Fig. 9. It is evident that the AMRs are not very large, which is different from the case when the impurities are fully polarized. For magnetization $\zeta < \zeta_0$, AMR is tiny when $\lambda < 1$ owing to the larger contribution from the magnetic scattering part. With enlarging the λ, the
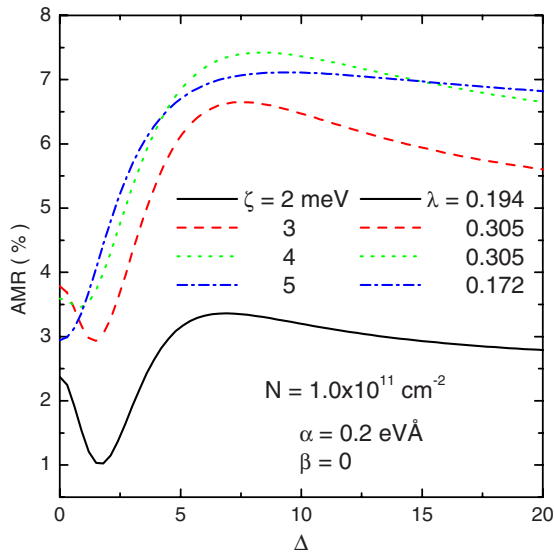
FIG. 10. (Color online) The peak value of the AMR near $0.1 < \lambda < 1$ for various magnetizations ($\zeta_0 < \zeta < \varepsilon_F$) is shown as functions of anisotropic constant Δ for pure Rashba model. The other parameters are the same as in Fig. 9.

contribution from the remote electric scattering becomes important, leading to the increment in AMR, and AMR finally saturates for very large λ. For middle magnetization $\zeta_0 < \zeta < \varepsilon_F$, the AMR shows a complicate behavior. The contribution from the magnetic (electric) scattering plays the leading role in the AMR for small (large) λ. For middle λ ($10^{-2} < \lambda < 10^2$), the contributions from the electric and magnetic parts to the AMR are comparable and an obvious competition occurs. With increasing the λ, the AMR first increases, then decreases, and enhances again. There is a peak of AMR at the position $0.1 < \lambda < 1$. In order to study the character of this peak, the AMRs are shown functions of λ for various anisotropic Δ at fixed magnetization in Fig. 9(d). It is seen clearly that the peak value ascends with anisotropic parameter but the position of the peak is almost unaffected. For large magnetization $\zeta > \varepsilon_F$, the AMR due to pure magnetic scattering is larger than the one due to pure remote electric scattering. Hence, with increasing the λ, the AMR drops.

Further, to demonstrate whether the AMR for $\zeta_0 < \zeta < \varepsilon_F$ can be large when two contributions are comparable, we also compute the peak value of AMR near the regime $0.1 < \lambda < 1$ versus the anisotropic constant Δ in Fig. 10. Unfortunately, the AMR is not very large even for large anisotropy, unlike the single-orientation model. The AMR may even decreases with the Δ and saturates at large one. We know that the XXZ model is the special case of XYZ model when the anisotropy is along the z direction. However, the study of AMR when the anisotropy is along the other direction shows that the AMR is also not very large and a similar behavior of AMR is obtained. Hence, when the magnetic impurities in magnetic materials are partly polarized, the large AMR ($\approx 200\%$) cannot be observed.

IV. CONCLUSIONS

We have proposed a kinetic equation approach to study the AMR in 2DEG with a combined Rashba and Dresselhaus SOC and an in-plane magnetization. Our model describes the case where the doped magnetic impurities are polarized partially in InAs quantum well, which is different from the previous fully polarized case. At the lowest order, these magnetic disorders give rise to a spontaneous magnetization. The remaining effect of magnetic impurities is included by considering the scattering between electron and impurity, modeled by XXZ or XYZ model. The microscopic mechanism of this AMR arises from the combined effect of SOC and polarized bands due to magnetization. This is different from the previous theoretical studies, where the polarized impurities instead of the polarized bands are responsible for the existence of AMR.

It is found that the Fermi contours of this single-particle Hamiltonian have a degenerate point for certain magnetization and direction of momentum, leading to novel property of AMR for both electric and magnetic scatterings. After averaging over the orientations of the local magnetic moments, the coherent superposition of electric and magnetic scattering amplitudes disappears in the scattering integral, which is valid even for the general XYZ model. The general argument could be made for the occurrence of AMR from the

kinetic equations. The destruction of the relation $v_\mu^x(k_x, k_y) = v_\mu^y(k_y, k_x)$ or $\rho_{\mu\mu}^x(k_x, k_y) = \rho_{\mu\mu}^y(k_y, k_x)$ may lead to the AMR. In the presence of combination of SOC and magnetization, it is obtained that both $v_\mu^x(k_x, k_y) \neq v_\mu^y(k_y, k_x)$ and $\rho_{\mu\mu}^x(k_x, k_y) \neq \rho_{\mu\mu}^y(k_y, k_x)$, resulting in the nonvanishing AMR even for electric collision. Nevertheless, the nonvertex and vertex parts of conductivities cancel each other for short-range one,[15] leading to disappearance of AMR. For identical coupling constants ($\alpha = \beta$), AMR vanishes completely for any scattering potential.

For electric collision, we consider both remote and background long-range potentials. The results show that the magnitude of AMR due to remote scattering is larger than background charged one. A sudden step of AMR appears near the regime $\zeta \approx \varepsilon_F$, which may reverse the sign of AMR. A small structure of AMR, which could be smoothed by the large distance of impurities, occurs near $\zeta \approx \zeta_0$. Both the magnitude and the sign of AMR could be tuned by adjusting the relative strength of two SOCs. In the presence of magnetic scattering, the AMR equals zero at vanishing magnetization for arbitrary magnitude of anisotropy Δ for XXZ model. Further, if the magnetization is smaller than the singular magnetization, the magnitude of AMR is tiny. A remarkable step structure also emerges while the sign of the AMR is always positive. The magnitude of AMR saturates at large anisotropic constant, especially, the maximum value of AMR could reach up to nearly 100% when the Fermi energy only crosses the majority band. In the presence of EMI scattering, the sign of the AMR is still positive even for $\zeta > \varepsilon_F$. At the same time, we adjust two scattering contributions and find that the magnitude of AMR is not very large, which is different from the single-orientation model. This is due to the vanishing of the coherent sum of two scattering parts when the magnetic impurities are partly polarized.

APPENDIX A: SELF-ENERGY

In this appendix, we give the expression of the self-energy in the helix basis in Eq. (17). Performing the integral of the solid angle Ω_M, the elements of the self-energy Σ are written as

$$\Sigma_{11}(\boldsymbol{k}) = \sum_{\boldsymbol{q}} \{a_1 G_{11}(\boldsymbol{q}) + a_2 G_{22}(\boldsymbol{q}) + id[G_{12}(\boldsymbol{q}) - G_{21}(\boldsymbol{q})]\},$$
(A1)

$$\Sigma_{12}(\boldsymbol{k}) = \Sigma_{21}^*(\boldsymbol{k})$$
$$= \sum_{\boldsymbol{q}} \{id[G_{11}(\boldsymbol{q}) - G_{22}(\boldsymbol{q})] + b_1 G_{12}(\boldsymbol{q}) + b_2 G_{21}(\boldsymbol{q})\},$$
(A2)

$$\Sigma_{11}(\boldsymbol{k}) = \sum_{\boldsymbol{q}} \{a_2 G_{11}(\boldsymbol{q}) + a_1 G_{22}(\boldsymbol{q}) - id[G_{12}(\boldsymbol{q}) - G_{21}(\boldsymbol{q})]\}.$$
(A3)

For shortness, here, the superscripts $(<, r, a)$ of self-energy and Green's function have been dropped. a_μ, b_μ, and d are factors depending on the scattering potentials

$$a_\mu = \frac{1}{6} v_M^2(\boldsymbol{k} - \boldsymbol{q})[2 + \Delta^2 + (-1)^\mu \Delta^2 \cos(\chi_{\boldsymbol{k}} - \chi_{\boldsymbol{q}})]$$
$$+ \frac{1}{2} v_N^2(\boldsymbol{k} - \boldsymbol{q})[1 - (-1)^\mu \cos(\chi_{\boldsymbol{k}} - \chi_{\boldsymbol{q}})],$$
(A4)

$$b_\mu = -\frac{1}{6} v_M^2(\boldsymbol{k} - \boldsymbol{q})[2 - \Delta^2 - (-1)^\mu \Delta^2 \cos(\chi_{\boldsymbol{k}} - \chi_{\boldsymbol{q}})]$$
$$+ \frac{1}{2} v_N^2(\boldsymbol{k} - \boldsymbol{q})[1 - (-1)^\mu \cos(\chi_{\boldsymbol{k}} - \chi_{\boldsymbol{q}})],$$
(A5)

$$d = \frac{1}{6}[\Delta^2 v_M^2(\boldsymbol{k} - \boldsymbol{q}) - 3 v_N^2(\boldsymbol{k} - \boldsymbol{q})]\sin(\chi_{\boldsymbol{k}} - \chi_{\boldsymbol{q}}).$$
(A6)

It is found that each element of the self-energy contains all the elements of the Green's function. However, the crossed term of two scattering strengths does not take place in these expressions.

APPENDIX B: KINETIC EQUATION FOR XYZ INTERACTION

Considering the general XYZ model for magnetic impurity scattering, the potential $u_M(\boldsymbol{r})$ takes the form

$$u_M(\boldsymbol{r}) = \sum_{\{\boldsymbol{R}_j, \theta_{Mj}, \varphi_{Mj}\}} J(\boldsymbol{r} - \boldsymbol{R}_j)[\Delta_x s_x S_x(\boldsymbol{R}_j, \theta_{Mj}, \phi_{Mj})$$
$$+ \Delta_y s_y S_y(\boldsymbol{R}_j, \theta_{Mj}, \phi_{Mj}) + \Delta_z s_z S_z(\boldsymbol{R}_j, \theta_{Mj}, \phi_{Mj})].$$
(B1)

Here $\Delta_x, \Delta_y, \Delta_z$ are the anisotropic constants. Hence, we get

$$u_M(\boldsymbol{r}) = \sum_{\{\boldsymbol{R}_j, \theta_{Mj}, \varphi_{Mj}\}} v_M(\boldsymbol{r} - \boldsymbol{R}_j) U_M^{XYZ}(\theta_{Mj}, \phi_{Mj})$$
(B2)

with the scattering strength $v_M(\boldsymbol{r} - \boldsymbol{R}_j) = J(\boldsymbol{r} - \boldsymbol{R}_j) S(\boldsymbol{R}_j)/2$ and the matrix $U_M^{XYZ}(\theta_{Mj}, \varphi_{Mj})$

$$U_M^{XYZ}(\theta_M, \phi_M) = \begin{pmatrix} \Delta_z \cos\theta_M & t(\theta_M, \phi_M) \\ t^*(\theta_M, \varphi_M) & -\Delta_z \cos\theta_M \end{pmatrix}.$$
(B3)

Here $t(\theta_M, \phi_M) = \sin\theta_M(\Delta_x \cos\phi_M - i\Delta_y \sin\phi_M)$. We would like to point out that for $\Delta_x = \Delta_y = 1$, the 2×2 matrix $U_M^{XYZ}(\theta_M, \phi_M)$ becomes $U_M(\theta_M, \phi_M)$. After applying the procedure of the average over the positions and the orientations of the local magnetic moments, the self-energy could be obtained. Finally, we get the kinetic equations. The kinetic equations are similar to Eqs. (19) and (20), only the $\Lambda_{\mu\mu'}(\boldsymbol{k}, \boldsymbol{q})$ and $\bar{\Lambda}_{\mu\mu'}(\boldsymbol{k}, \boldsymbol{q})$ are replaced by $\Lambda_{\mu\mu'}^{XYZ}(\boldsymbol{k}, \boldsymbol{q})$ and $\bar{\Lambda}_{\mu\mu'}^{XYZ}(\boldsymbol{k}, \boldsymbol{q})$. The $\Lambda_{\mu\mu'}^{XYZ}(\boldsymbol{k}, \boldsymbol{q})$ and $\bar{\Lambda}_{\mu\mu'}^{XYZ}(\boldsymbol{k}, \boldsymbol{q})$ have the form

$$\Lambda_{\mu\mu'}^{XYZ}(\boldsymbol{k},\boldsymbol{q}) = v_N^2(\boldsymbol{k}-\boldsymbol{q})[1+(-1)^{\mu+\mu'}\cos(\chi_k-\chi_q)]$$

$$+\frac{1}{3}v_M^2(\boldsymbol{k}-\boldsymbol{q})\{\Delta_x^2[1-(-1)^{\mu+\mu'}\cos(\chi_k+\chi_q)]$$

$$+\Delta_y^2[1+(-1)^{\mu+\mu'}\cos(\chi_k+\chi_q)]$$

$$+\Delta_z^2[1-(-1)^{\mu+\mu'}\cos(\chi_k-\chi_q)]\}, \quad (B4)$$

$$\bar{\Lambda}_{\mu\mu'}^{XYZ}(\boldsymbol{k},\boldsymbol{q}) = (-1)^{\mu'}\frac{1}{3}\{3v_N^2(\boldsymbol{k}-\boldsymbol{q})\sin(\chi_k-\chi_q)-v_M^2(\boldsymbol{k}-\boldsymbol{q})$$

$$\times[\Delta_x^2\sin(\chi_k+\chi_q)-\Delta_y^2\sin(\chi_k+\chi_q)$$

$$+\Delta_z^2\sin(\chi_k-\chi_q)]\}. \quad (B5)$$

For this general XYZ model, these quantities depend on both $\chi_k+\chi_q$ and $\chi_k-\chi_q$ through a cosine or sine function. However the coherent sum between electric and magnetic scattering potentials still does not exist.

The scattering-related quantities $\Lambda_{\mu\mu'}^{XYZ}(\boldsymbol{k},\boldsymbol{q})$ depend on $\chi_k+\chi_q$ hence AMR may exist for pure magnetic scattering in the absence of magnetization. For pure Rashba model and short-range scattering, $v_M^2(\boldsymbol{k}-\boldsymbol{q})=v_0^2$, the analytical solution of kinetic equation could be obtained as

$$\rho_{\mu\mu}^x(\boldsymbol{k}) = -\frac{e}{mv_0^2}\frac{3}{(\Delta_x^2+\Delta_y^2+\Delta_z^2)(3\Delta_x^2+\Delta_y^2+3\Delta_z^2)}$$

$$\times\left[(-1)^\mu\alpha(\Delta_x^2-\Delta_y^2+\Delta_z^2)+(3\Delta_x^2+\Delta_y^2+3\Delta_z^2)\right.$$

$$\times\left.\sqrt{\alpha^2+\frac{2\varepsilon_F}{m}}\right]\cos\theta\,\delta(\varepsilon_{k\mu}-\varepsilon_F), \quad (B6)$$

$$\rho_{\mu\mu}^y(\boldsymbol{k}) = -\frac{e}{mv_0^2}\frac{3}{(\Delta_x^2+\Delta_y^2+\Delta_z^2)(\Delta_x^2+3\Delta_y^2+3\Delta_z^2)}$$

$$\times\left[(-1)^\mu\alpha(\Delta_y^2-\Delta_x^2+\Delta_z^2)+(\Delta_x^2+3\Delta_y^2+3\Delta_z^2)\right.$$

$$\times\left.\sqrt{\alpha^2+\frac{2\varepsilon_F}{m}}\right]\sin\theta\,\delta(\varepsilon_{k\mu}-\varepsilon_F). \quad (B7)$$

Thus the longitudinal conductivities take the form

$$\sigma_{xx} = \frac{3e^2}{m\pi v_0^2}\left(\frac{\varepsilon_F}{\Delta_x^2+\Delta_y^2+\Delta_z^2}+\frac{m\alpha^2}{3\Delta_x^2+\Delta_y^2+3\Delta_z^2}\right), \quad (B8)$$

$$\sigma_{yy} = \frac{3e^2}{m\pi v_0^2}\left(\frac{\varepsilon_F}{\Delta_x^2+\Delta_y^2+\Delta_z^2}+\frac{m\alpha^2}{\Delta_x^2+3\Delta_y^2+3\Delta_z^2}\right). \quad (B9)$$

Hence, the resultant AMR is directly given by

$$AMR = \frac{2m\alpha^2(\Delta_x^2-\Delta_y^2)(\Delta_x^2+\Delta_y^2+\Delta_z^2)}{\varepsilon_F F_1+m\alpha^2 F_2} \quad (B10)$$

here $F_1=(3\Delta_x^2+\Delta_y^2+3\Delta_z^2)(\Delta_x^2+3\Delta_y^2+3\Delta_z^2)$ and $F_2=(\Delta_x^2+\Delta_y^2+\Delta_z^2)(2\Delta_x^2+2\Delta_y^2+3\Delta_z^2)$. AMR is nonzero for general XYZ model in the absence of magnetization. Nevertheless, it vanishes for XXZ model or for the spin-degenerate system. The XYZ model when $\Delta_x\neq\Delta_y$ breaks the in-plane symmetry of

the scattering potential, which may lead to anisotropic electron lifetimes. Hence, AMR occurs in the absence of in-plane magnetization. When all the moments of magnetic impurities align along x (y) direction, i.e., $\theta_M=\pi/2$, $\phi_M=0$, ($\theta_M=\pi/2$, $\phi_M=\pi/2$), the resultant AMR is consistent with the previous study.[11] On the other hand, if the orientations of local magnetic moments are still random, but only one in-plane coupling strength is nonzero, i.e., $\Delta_x=1$, $\Delta_y=\Delta_z=0$ or $\Delta_y=1$, $\Delta_x=\Delta_z=0$, the obtained AMR is still different from the one of the single-orientation model. For example, for $\Delta_x=1$, $\Delta_y=\Delta_z=0$, the longitudinal conductivities are written as

$$\sigma_{xx} = \frac{3e^2}{m\pi v_0^2}\left(\frac{\pi N}{m}-\frac{2m\alpha^2}{3}\right), \quad (B11)$$

$$\sigma_{yy} = \frac{3e^2N}{m^2v_0^2}. \quad (B12)$$

They are three times as large as the results of single-orientation model.[11] This is due to the randomicity of the orientations of impurity spins, which can be seen from the expression of the $\Lambda_{\mu\mu'}^{XYZ}(\boldsymbol{k},\boldsymbol{q})$. The similar result can be obtained for the case $\Delta_y=1$, $\Delta_x=\Delta_z=0$. Therefore, our model is significantly different from the single-orientation model and they are relevant to different physical systems.

APPENDIX C: ANALYTICAL RESULT OF AMR FOR PURE MAGNETIC SCATTERING WHEN ONLY THE MAJORITY BAND IS OCCUPIED

For this one band model ($\zeta>\varepsilon_F$), one only needs the distribution function $\rho_{11}^i(\boldsymbol{k})$. In order to determine this distribution, we assume the solution of Eq. (24) at zero temperature has the form $\rho_{11}^i(\boldsymbol{k})=f^i(\theta)\delta(\varepsilon_{k1}-\varepsilon_F)$. Here $f^i(\theta)$ only relies on the polar angle of momentum. As a result, all the corresponding physical quantities should be calculated at the Fermi surface. Further, the weak SOC is assumed. To first order in $m\alpha^2/\zeta$, the magnitude of angle-dependent Fermi momentum, $k_1(\theta)$, is expressed as

$$k_1(\theta) = \sqrt{2m(\zeta+\varepsilon_F)}-m\alpha\sin\theta+\left(\frac{m}{2}\right)^{3/2}$$

$$\times\frac{\zeta+\zeta\cos^2\theta+2\varepsilon_F\cos^2\theta}{\zeta\sqrt{\zeta+\varepsilon_F}}\alpha^2. \quad (C1)$$

At the same time, two components of the group velocity at the Fermi surface for weak spin-orbit splitting are written as

$$v_{k_11}^x = \sqrt{\frac{2(\zeta+\varepsilon_F)}{m}}\cos\theta-\frac{1}{2}\alpha\sin2\theta+\frac{1}{16\zeta}\alpha^2\sqrt{\frac{2m}{\zeta+\varepsilon_F}}$$

$$\times[-(9\zeta+10\varepsilon_F)\cos\theta+(\zeta+2\varepsilon_F)\cos3\theta], \quad (C2)$$

$$v_{k_1 1}^{y} = \sqrt{\frac{2(\zeta + \varepsilon_F)}{m}} \sin\theta + \frac{1}{2}\alpha(1 + \cos 2\theta)$$
$$+ \frac{1}{16\zeta}\alpha^2 \sqrt{\frac{2m}{\zeta + \varepsilon_F}}[(5\zeta + 2\varepsilon_F)\sin\theta + (\zeta + 2\varepsilon_F)\sin 3\theta]. \tag{C3}$$

It is found that the components of velocity at Fermi surface depend not only on θ but also on 2θ and 3θ, through not only a cosine function but also a sine function. Meanwhile, to the first order in $m\alpha^2/\zeta$ and $\Delta^2 m\alpha^2/\zeta$, the quantity $\Lambda_{11}(\mathbf{k},\mathbf{q})$ at the Fermi surface can also be obtained. However, its expression is too lengthy and we don't write it down here. Further, we assume $f^i(\theta) = f_0^i(\theta) + \alpha f_1^i(\theta) + \alpha^2 f_2^i(\theta)$. Considering the fact that both the left hand side and the right-hand side of Eq. (24) are periodic functions of θ, the $f_\nu^i(\theta)$ ($\nu = 0, 1, 2$) should have the form

$$f_\nu^i(\theta) = A_\nu^i(0) + \sum_{n=1}^{\infty} A_\nu^i(n)\cos n\theta + \sum_{n=1}^{\infty} B_\nu^i(n)\sin n\theta. \tag{C4}$$

The coefficients of the Fourier series are determined by Eq. (24). One finds that only the following coefficients are non-zero:

$$A_0^x(1) = B_0^y(1) = \frac{-6e}{\sqrt{2}mv_0^2}\frac{\sqrt{\zeta + \varepsilon_F}}{m}, \tag{C5}$$

$$B_1^x(2) = -A_1^y(2) = \frac{3e}{2mv_0^2}, \tag{C6}$$

$$A_2^x(1) = \frac{3e}{8\sqrt{2}v_0^2}\frac{18\Delta^2(\zeta + \varepsilon_F)^2 + \zeta(17\zeta + 18\varepsilon_F)}{\zeta^2\sqrt{m(\zeta + \varepsilon_F)}}, \tag{C7}$$

$$B_2^y(1) = \frac{9e}{8\sqrt{2}v_0^2}\frac{2\Delta^2(\zeta + \varepsilon_F)^2 + \zeta(\zeta + 2\varepsilon_F)}{\zeta^2\sqrt{m(\zeta + \varepsilon_F)}}, \tag{C8}$$

$$A_2^x(3) = B_2^y(3) = \frac{3e}{8\sqrt{2}v_0^2}\frac{2\Delta^2(\zeta + \varepsilon_F)^2 - \zeta(\zeta + 2\varepsilon_F)}{\zeta^2\sqrt{m(\zeta + \varepsilon_F)}}. \tag{C9}$$

Actually, the coefficients $A_2^x(3)$ and $B_2^y(3)$ are not necessary for the calculation of conductivities to the first order in $m\alpha^2/\zeta$ due to the vanishing integrations of angle, such as $\int_0^{2\pi} d\theta \cos\theta \cos 3\theta$. Finally, we obtain the longitudinal conductivities for weak SOC

$$\sigma_{xx} = \frac{3e^2(\zeta + \varepsilon_F)}{2\pi}\tau - \frac{3e^2m\alpha^2\tau}{16\pi\zeta^2}$$
$$\times [9\Delta^2(\zeta + \varepsilon_F)^2 + 4\zeta(\zeta + 2\varepsilon_F)], \tag{C10}$$

$$\sigma_{yy} = \frac{3e^2(\zeta + \varepsilon_F)}{2\pi}\tau - \frac{3e^2m\alpha^2\tau}{16\pi\zeta^2}\times[3\Delta^2(\zeta + \varepsilon_F)^2 - 4\zeta^2]. \tag{C11}$$

Here the relaxation time τ is defined as $\tau = 1/(mv_0^2)$. Obviously, $\sigma_{yy} > \sigma_{xx}$ and both of them are quadratically related to the spin-orbit interaction for fixed Fermi energy. With increasing the coupling strength α, the σ_{xx} decreases, while the σ_{yy} may increases. For vanishing SOC, $\sigma_{xx} = \sigma_{yy} = 3e^2(\zeta + \varepsilon_F)\tau/2\pi$, which differs from the Drude conductivity. We should note that the above conductivities cannot be reduced to the nonmagnetic case since the XXZ model for magnetic disorder is not reducible to that for nonmagnetic one. Finally, we get the AMR Eq. (33) for $m\alpha^2/\zeta \ll 1$ and $\Delta^2 m\alpha^2/\zeta \ll 1$.

---

*cmwangsjtu@gmail.com

[1] W. Thomson, Proc. R. Soc. London **8**, 546 (1857).

[2] I. Žutić, J. Fabian, and S. Das Sarma, Rev. Mod. Phys. **76**, 323 (2004).

[3] T. Jungwirth, J. Sinova, J. Mašek, J. Kučera, and A. H. Mac-Donald, Rev. Mod. Phys. **78**, 809 (2006).

[4] H. X. Tang, R. K. Kawakami, D. D. Awschalom, and M. L. Roukes, Phys. Rev. Lett. **90**, 107201 (2003).

[5] K. Y. Wang, K. W. Edmonds, R. P. Campion, L. X. Zhao, C. T. Foxon, and B. L. Gallagher, Phys. Rev. B **72**, 085201 (2005).

[6] A. W. Rushforth, K. Výborný, C. S. King, K. W. Edmonds, R. P. Campion, C. T. Foxon, J. Wunderlich, A. C. Irvine, P. Vašek, V. Novák, K. Olejník, J. Sinova, T. Jungwirth, and B. L. Gallagher, Phys. Rev. Lett. **99**, 147207 (2007).

[7] K. Pappert, C. Gould, M. Sawicki, J. Wenisch, K. Brunner, G. Schmidt, and L. W. Molenkamp, New J. Phys. **9**, 354 (2007).

[8] R. R. Gareev, A. Petukhov, M. Schlapps, J. Sadowski, and W. Wegscheider, Appl. Phys. Lett. **96**, 052114 (2010).

[9] J. Smit, Physica **17**, 612 (1951).

[10] T. McGuire and R. Potter, IEEE Trans. Magn. **11**, 1018 (1975).

[11] M. Trushin, K. Výborný, P. Moraczewski, A. A. Kovalev, J. Schliemann, and T. Jungwirth, Phys. Rev. B **80**, 134405 (2009).

[12] C. M. Wang and M. Q. Pang, EPL **88**, 27005 (2009).

[13] R. Raimondi, M. Leadbeater, P. Schwab, E. Caroti, and C. Castellani, Phys. Rev. B **64**, 235110 (2001).

[14] The high-order contribution of short-range nonmagnetic scattering can lead to nonvanishing AMR but its magnitude is very small. See A. A. Kovalev, Y. Tserkovnyak, K. Výborný, and J. Sinova, Phys. Rev. B **79**, 195129 (2009).

[15] T. Kato, Y. Ishikawa, H. Itoh, and J. I. Inoue, Phys. Rev. B **77**, 233404 (2008).

[16] J. I. Inoue, T. Kato, Y. Ishikawa, H. Itoh, G. E. W. Bauer, and L. W. Molenkamp, Phys. Rev. Lett. **97**, 046604 (2006).

[17] S. Y. Liu and X. L. Lei, Phys. Rev. B **72**, 195329 (2005).

[18] C. M. Wang, M. Q. Pang, S. Y. Liu, and X. L. Lei, Phys. Lett. A **374**, 1286 (2010).

[19] M. Poggio, R. C. Myers, N. P. Stern, A. C. Gossard, and D. D. Awschalom, Phys. Rev. B **72**, 235313 (2005).

[20] S. Sanvito, P. Ordejón, and N. A. Hill, Phys. Rev. B **63**, 165206 (2001).

[21] S. Das Sarma, E. H. Hwang, and A. Kaminski, Phys. Rev. B **67**, 155201 (2003).

[22] R. Žitko, R. Peters, and Th. Pruschke, Phys. Rev. B **78**, 224404 (2008).

[23] A. Schiller and L. De Leo, Phys. Rev. B **77**, 075114 (2008).

[24] P. Wang, Y.-Q. Li, and X. Zhao, Phys. Rev. B **75**, 075326 (2007).

[25] L. Ren, J. Phys.: Condens. Matter **20**, 075216 (2008).

[26] L. Ren, Phys. Lett. A **372**, 4307 (2008).

[27] D. V. Baxter, D. Ruzmetov, J. Scherschligt, Y. Sasaki, X. Liu, J. K. Furdyna, and C. H. Mielke, Phys. Rev. B **65**, 212407 (2002).

[28] W. Limmer, M. Glunk, J. Daeubler, T. Hummel, W. Schoch, R. Sauer, C. Bihler, H. Huebl, M. S. Brandt, and S. T. B. Goennenwein, Phys. Rev. B **74**, 205205 (2006).

[29] A. W. Rushforth, K. Výborný, C. S. King, K. W. Edmonds, R. P. Campion, C. T. Foxon, J. Wunderlich, A. C. Irvine, V. Novák, K. Olejník, A. A. Kovalev, J. Sinova, T. Jungwirth, and B. L. Gallagher, J. Magn. Magn. Mater. **321**, 1001 (2009).

[30] K. Výborný, J. Kučera, J. Sinova, A. W. Rushforth, B. L. Gallagher, and T. Jungwirth, Phys. Rev. B **80**, 165204 (2009).

[31] K. Výborný, A. A. Kovalev, J. Sinova, and T. Jungwirth, Phys. Rev. B **79**, 045427 (2009).

[32] D. Grundler, Phys. Rev. Lett. **84**, 6074 (2000).

[33] P. Schwab and R. Raimondi, Eur. Phys. J. B **25**, 483 (2002).

[34] H. Haug and A.-P. Jauho, *Quantum Kinetics in Transport and Optics of Semiconductors* (Springer, New York, 1996).

[35] X. L. Lei, J. L. Birman, and C. S. Ting, J. Appl. Phys. **58**, 2270 (1985).

[36] J. C. Cao, X. L. Lei, A. Z. Li, M. Qi, and H. C. Liu, Semicond. Sci. Technol. **17**, 215 (2002).

[37] C. M. Wang, S. Y. Liu, Q. Lin, X. L. Lei, and M. Q. Pang, J. Phys.: Condens. Matter **22**, 095803 (2010).